 doi:10.20944/preprints202210.0354.v1

Article

Mini-Spidroin Filamentation in Different Methanol Concentration Coagulation Bath

Jie Zhang[1], Mengxin Gong[2], Qiupin Jia[1] and Qing Meng[1,2] ID

1. College of Biological Science and Medical Engineering, Donghua University, Shanghai 201600, China
2. College of Life and Geographic Sciences, Kashi University, Kashi, Xinjiang, 844000, China

Abstract:

Spider silk has excellent strength and elasticity in natural, researchers have been working for decades try to achieve natural spider silk outstanding mechanical properties using recombinant spider silk protein (spidroin) through artificial spinning. In this work, we chose wet spinning method to explore the relationship between concentration of coagulation bath and fiber performance. It was found that the concentration of methanol has important effect on fiber continuity, diameter and mechanical properties. Lower concentration favors spinning continuous thinner, fibers with high strain. Secondary stretching benefits spinning silk fibers with stable mechanical properties, and thermal stability. Through applying different methanol concentration and additional stretching, we obtained silk fibers with Young's modulus of 3.052± 2.626 GPa, stress of 25.3944 ± 17.48 MPa, and strain of 140 ± 95.4%.

Keywords: Spidroin; wet spinning; methanol

1. Introduction

The orb-web spiders are efficient producers of different types of silks, which were used for different biological purposes from constituting the orb-web to the construction of the egg's cocoon, that are characterized by their diverse chemical compositions, structure, and function [1]. Pyriform silk serves as the junction former in spider webs and is the fibrous component of a two-part system called an attachment disc [17]. The other part of the attachment disc is a glue-like material that is produced deeper in the gland and coated onto the pyriform silk fiber during spinning [2]. The role of pyriform nonrepetitive domains function similarly to those in other silk types, for simplicity of recombinant protein production and to allow elaboration of features inherent to pyriform spidroin. Pyriform silk is used to create disks for attachment of silk to various substrate, for example as anchor points for the dragline, the frame of a web, or a sheet, or to attach egg cases to a surface [3].

The spinning of silk starts with a highly concentrated protein solution produced in a sac in the initial region of the silk glands. The sac is anchored by the funnel to an S-shaped duct that tapers down to the spigot [14]. The initially isotropic protein solution acquires a liquid crystal structure in the funnel, so that it can flow easily through the narrow duct [15]. The liquid crystal structure could also promote the pre-alignment of the fibers prior to full fiber formation. The fiber is formed from the solution in the third limb of the duct, as is seen from the separation of the lateral surface of the fiber from the walls of the duct, and emerges through the lips of the spigot [16]. The identification of structures along the duct and in the spigot responsible for recovering water initially present in the aqueous solution suggests that water content might be a critical parameter during spinning [4].

Most of the techniques that have been applied to form fibers from a silk solution have been based on solvent extrusion, wet-spinning through a coagulation bath, electrospinning, and microfluidic approaches, sometimes using organic solvents [18]. On an industrial scale, fibers are typically produced via a melt-extrusion process (dry-spinning) or spinning in to a precipitation bath (wet-spinning), while smaller fibers with single micron diameters are fabricated using electrospinning and microfluidic spinning on a lab scale [5]. Wet spinning is a manufacturing method for creating polymer fibers from a solution. During wet spinning, the spinneret is submerged in a chemical bath and filaments subsequently solidify and precipitate from the polymer solutions [10]. Compared to electrospinning, conventional wet spinning has important advantages such as low cost, mild conditions and allows for the possibility

 doi:10.20944/preprints202210.0354.v1

of spinning various bioinks composed of highly biocompatible polymers based on native extracellular matrix components loaded with cells [6].

In previous work, the recombinant spidroin silk has been used in electrospinning method with PCL, it can improve the strength of the compound membrane [20]. There have been reported that the recombinant spidroin were spinning in formic acid [13]. Here we tried to use another method to improve the elasticity of the fiber.

2. Material and method

2.1. Protein expression and purification

The protein was expressed in *E. coli* BL 21 (DE3) cells, induced at 16℃, and purified from inclusion bodies.

2.2. Circular dichroism spectroscopy (CD)

A dope sample was prepared at 10% w/v. Spectra of the recombination spidroin was recorded in 1nm bandwidth from 190 nm to 260 nm at 20±1℃ with a chirascan spectrometer (J-815, JASCO Japan). Blank subtraction was performed, and mean residue ellipticity was calculated and averaged from two repetitions. To obtain values for the relative percentage of each type of secondary structure present, CD data in [θ] format were deconvoluted using the BeStSel algorithm [7] (http://bestsel.elte.hu/index.php).

2.3. Fiber spinning and post-spin stretching

The protein lyophilized powder of NRC was dissolved in hexafluoroisopropanol (HFIP) with the concentration of 10% (w/v), the solution was stirred with a magnetic stirrer (Sangon biotech, Shanghai Co., Ltd.). Then transfer the spinning solution to a 1 mL syringe with a needle (30 μm diameter) and injected into a coagulation bath by a pump, the coagulation bath were different concentrations of methanol, shown in Table 1. Fibers were spun at a 0.2-0.3 mL/h spinning rate in the bath via a digital-controlled device containing scroll in air at room temperature. The fibers were collected on a 30 mm diameter scroll covered with a black cardboard cartridge by transparent adhesive tape, the scroll rotated 30-35 rpm/min. The linear distance between the fiber from coagulation bath and the reel for fiber collection was about 10cm (as shown in Figure 1A). Post-spin stretching of spidroin fiber collected in air and in 1% methanol coagulation bath, respectively, the diameter of the scroll and scroll rotated speed of post-spin stretched was 10 mm and 87-90 rpm/min, as shown in Figure 1B and 1C.

The overall spinning process was carried out at 25℃ and 30%--50% humidity. The fibers then dry out at the same room environment as above.

Preprints (www.preprints.org) | NOT PEER-REVIEWED | Posted: 24 October 2022 doi:10.20944/preprints202210.0354.v1

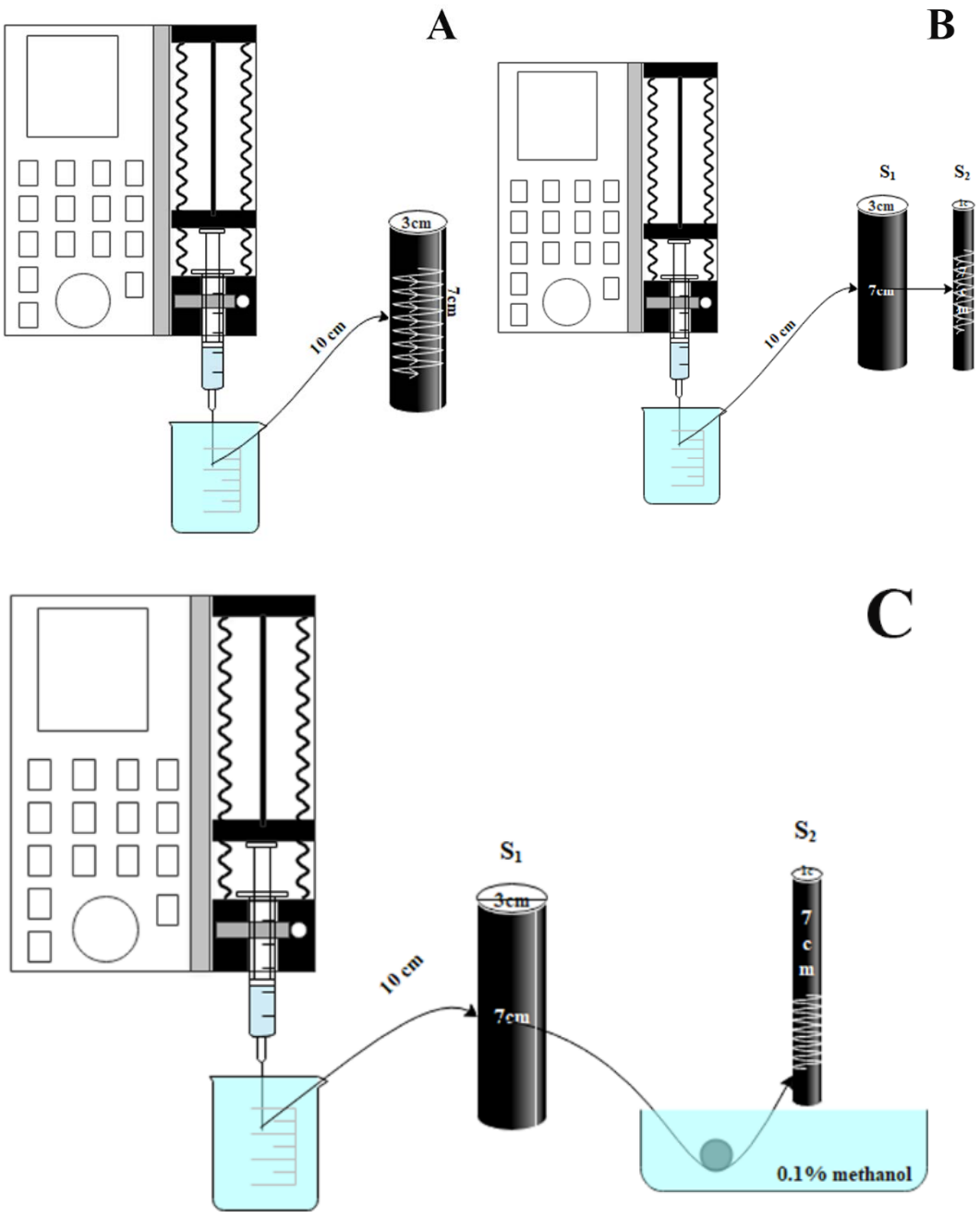

Figure 1: A: Schematic diagram of wets spinning, B: Wet spinning and post-spin stretching in air, C: Wet-spinning and post-spin stretching in methanol.

Table 1. The volume ratio of methanol in coagulation bath

Sample	V (Methanol) : V (Total)
a	1 : 2
b	1 : 5
c	1 : 10
d	1 : 50
e	1 : 100
f	1 : 100
g	1 : 100

 doi:10.20944/preprints202210.0354.v1

2.4. Morphology analysis of fibers

The morphology of spinning fibers was imaged by microscope (Leica, Germany), then analyzed by scanning electron microscope (SEM) system operating at 10 kV acceleration voltage at room temperature (FlexSEM1000, Hitachi, Japan). The fibers were fixed on a SEM plate with conducting resin followed by gold spray for 40 s.

Light microscopy images were collected using a Leica Las 4.12 inverted microscope equipped with a DFC Twain camera from Imagingsource. It was taken 10 pictures per silk, the silk in each picture was measured about 100 times.

2.5. FTIR

The mechanical structures of different fibers were detected using a FTIR spectrometer (NEXUS-670, Thermo, USA) at room temperature. All spectra were acquired in the spectral range of 4000-500 cm^{-1} with the resolution of 4 cm^{-1}. The amide I band (1600-1700 cm^{-1}) was selected for quantitative analysis of the secondary structure of spidroin fiber samples. The spectra were smoothed to remove the influence of vapor, corrected by background calibration and normalization.

2.6. Thermogravimetric analysis (Tg)

Thermogravimetric analysis (TGA) of the silk fibers was investigated with a TA instruments NETZSCH TG 209F1 (Netzsch, Germany). 2.5 milligrams of all different fibers were heated from 30℃ to 600℃ at a heating rate of 10 K/min. The percentage of mass change was recorded during heating process.

2.7. Mechanical test

Fibers were examined and diameters were determined as described in 2.4. Fibers were placed in the middle of a squared-shaped paper frame (Inner:1 cm×1 cm, outer: 1.5 cm×1.5cm) with each end of fiber taped on the frame to create a 1 cm long fiber for mechanical testing. Right before mechanical testing, the side of paper frame between the two ends of fibers was cut to allow free stretching of fibers. Mechanical testing was used a T150 universal test machine (UTM, KLA-Tencor Inc., Oak Ridge, USA) with a strain rate of 10-3 mm/s at room temperature.

2.8. Statistical analysis

The silk fibers were compared statistically using a ANOVA (analysis of variance) and student's t-test. $p>0.05$, means no difference, $0.05<p<0.01$ means difference, $p<0.01$ means significant difference.

3. Result and discussion

3.1. Protein purification and silk spinning

Preprints (www.preprints.org) | NOT PEER-REVIEWED | Posted: 24 October 2022 doi:10.20944/preprints202210.0354.v1

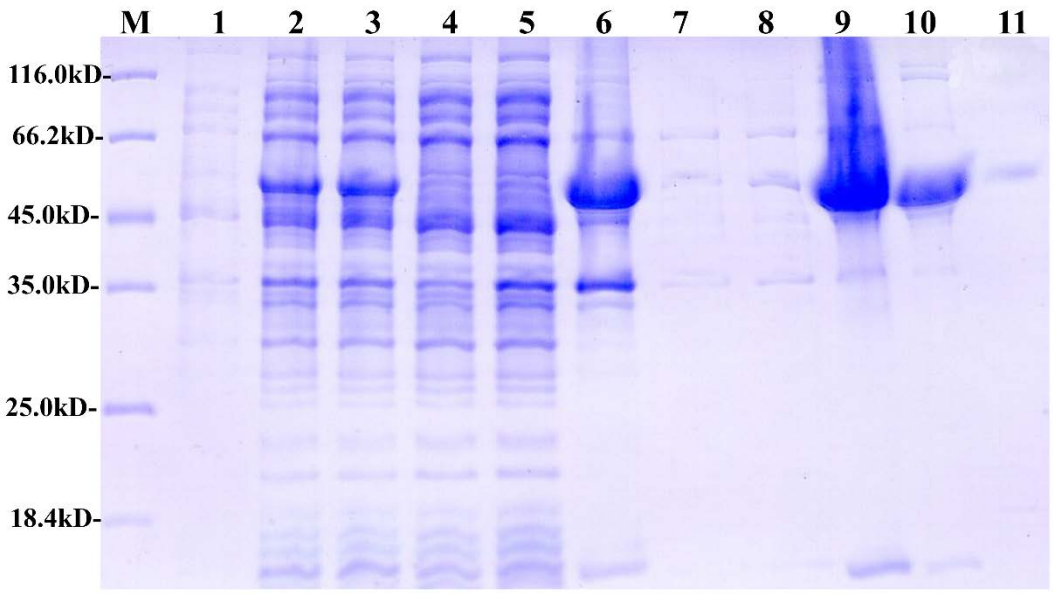

Figure 2: SDS-PAGE of recombinant spidroin purification. 1：Before induction, 2: 16℃ induction, 3: 16℃ induction-IPTG, 4: Supernatant, 5: Supernatant, 6: Precipitate, 7: Supernatant after rinsing, 8: Supernatant after rinsing, 9: Precipitate after rinsing, 10: Supernatant after lysis, 11: Precipitate after lysis.

The recombinant spidroin was expressed in inclusion bodies, then purified with urea. The purity of the protein can reach about 95% after purified and dialyzed in pure water.

This recombinant spidroin powder insoluble in acetic acid, formic acid and isopropanol, but soluble in HFIP. The spinning dope with a concentration of 10% (w/v) coagulate into a white mass at the end of needle in a pure methanol, as added the deionized water 10% (v/v) each time it can form fiber until the ratio was 5/9 ($V_{methanol}/V_{total\ volume}$), but the fiber couldn't form continuously. The spinning dope can filament well continuity as the methanol concentration decreased, while in pure deionized water it just like the spinning dope was being dissolved. The secondary stretching from the 1% methanol coagulation bath in the air (Figure 1B) and the solution as the coagulation bath (Figure 1C), the secondary stretching fibers were rotated in a scroll with the diameter of 10mm and speed of 90rpm. The distance between fiber from the coagulation and the scroll for fiber collection was about 10cm。

We choose methanol as the coagulation bath due to that monohydric alcohol has a strong ability to induce rapid conformation transition of silk protein and promote β-sheet formation [8]. Methanol or ethanol induce a too rapid conformation transition from random coil/ helix to β-sheet structure [9].

3.2. Morphology of fibers

3.2.1 Diameter of the fibers

Due to the fiber measurement started from the fiber could be picked out from the coagulation bath surface till it broken itself, the range of fiber diameter was higher. While it can also observed (Figure 3) that fiber's average diameter decreased as the coagulation bath concentration decreased, from about 21μm of 1:2 to about 14 μm of 1:100 ($V_{methanol}/V_{total\ volume}$). The diameter of secondary stretching fibers was steadily in air than in the 0.1% methanol. It means the concentration of coagulation bath methanol has no obvious effect on the fibers' secondary structure.

3.2.2 Morphology of fibers

The morphology of all fibers seems smooth under microscopy. While in SEM vision (Figure 4), the fibers of 1:2, 1:5, 1:10, and 1:50 ($V_{methanol}/V_{total\ volume}$) have preferential axial orientation fissures and grooves, induced by the spinning process and the concentration of methanol. As the concentration of methanol decreased to 1:100, the morphology of the fiber was smooth without

Preprints (www.preprints.org) | NOT PEER-REVIEWED | Posted: 24 October 2022 doi:10.20944/preprints202210.0354.v1

fissures in a field of view magnified by 2000×. The same field of view appears in both secondary stretching in air and in 0.1% methanol. The morphology of the fiber was worse at the high methanol concentration 1:2 compared with 1:5 one in the coagulation bath. In addition, clear micro-voids and grooves were seen in fiber formed in the 1:2 methanol coagulation bath. While as the concentration of methanol in coagulation bath decreased, the groove and fissure became smaller. This may due to the quick conformation transition of silk fibroin and fast water removal from the fiber in high methanol concentration coagulation bath. After post-drawing either in air or in 0.1% methanol, the fiber surface became smoother, showing a more uniform surface morphology. It was attributed to uniform molecular chain alignment during the postdraw process. However, due to the slightness of silk fiber, when immersed in methanol solution it usually solidified and break at the edge of the tank.

3.2.3 Cross-section

The fracture of the fiber spun in 1:2, 1:5 1:10, 1:50 methanol coagulation bath were found at the sample preparation, no fracture found with the 1:100 and the secondary stretching fibers (Figure 5). There were no obvious voids in neither high methanol concentration nor low concentration coagulation bath. The irregular shape and surface found in the SEM may be caused by the fiber broken.

The morphology of wet-spun fibers also affected by the coagulation kinetics. Usually, slow solvent diffusion leads to uniform porous structures, solvent system, temperature, polymeric concentration and molecular weight and the presence of additives in the solution and coagulation bath, nozzle diameter and injection rate, can also significantly affect the kinetics of coagulation [10].

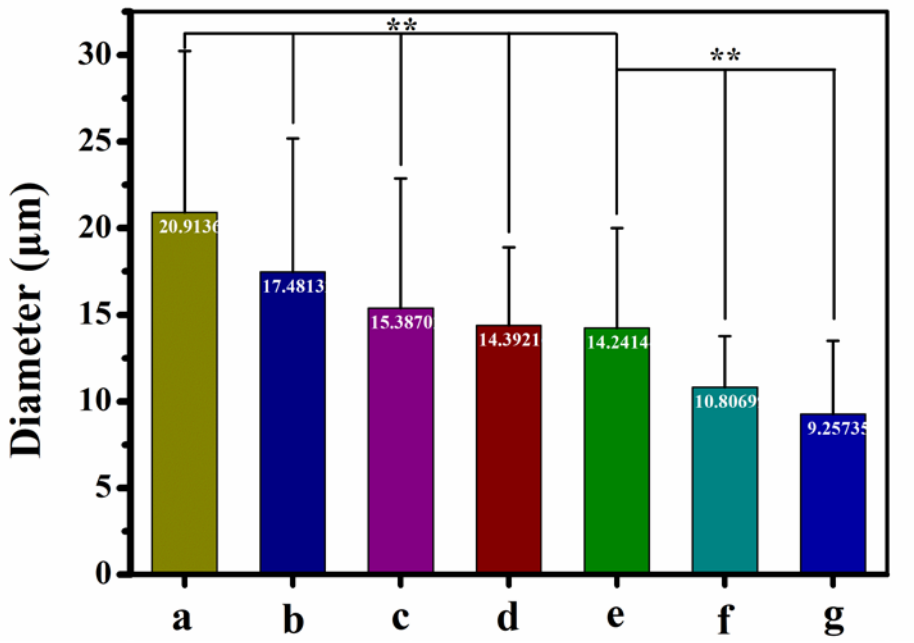

Figure 3: The diameter of spinning fibers in different coagulation bath and secondary stretching. a: V(Methanol)/ V(Total)=1:2, b: V(Methanol)/ V(Total)=1:5, c: V(Methanol)/ V(Total)=1:10, d: V(Methanol)/ V(Total)=1:50, e: V(Methanol)/ V(Total)=1:100, f: V(Methanol)/ V(Total)=1:100 and secondary stretching in air, g: V(Methanol)/ V(Total)=1:100 and secondary stretching in 0.1% methanol.

 doi:10.20944/preprints202210.0354.v1

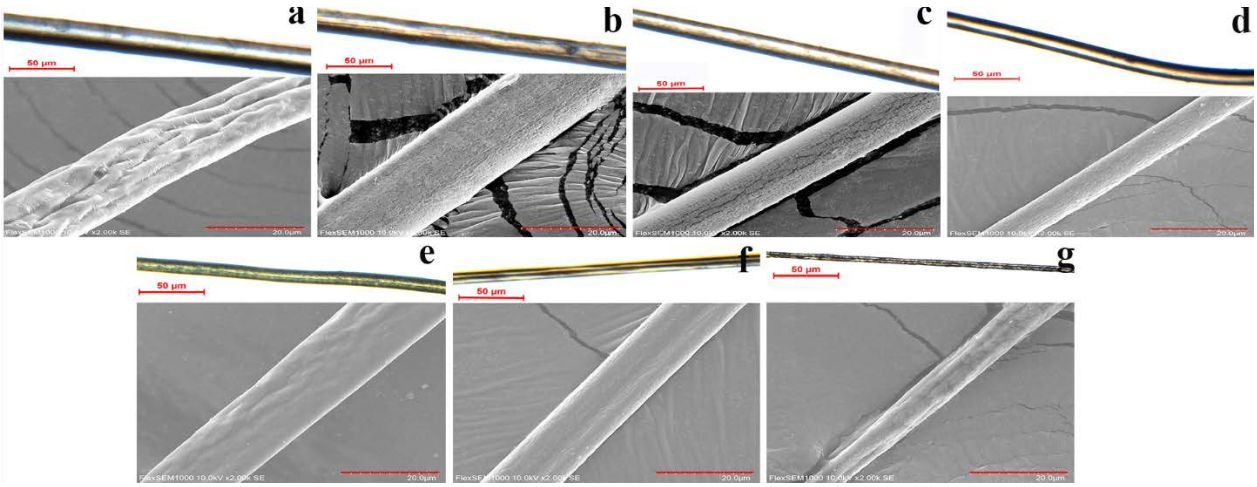

Figure 4: Surface morphology of spinning silk in different coagulation bath (a-e), and secondary stretching in air (f) or in methanol (g). Coagulation bath concentration: a: V(Methanol)/ V(Total)=1:2, b: V(Methanol)/ V(Total)=1:5, c: V(Methanol)/ V(Total)=1:10, d: V(Methanol)/ V(Total)=1:50, e: V(Methanol)/ V(Total)=1:100, f: V(Methanol)/ V(Total)=1:100, g: V(Methanol)/ V(Total)=1:100. The upper part of a-g was observed under the microscope, the bottom part was observed under SEM. The scale bar was 50μm in microscope picture, 20 μm in SEM.

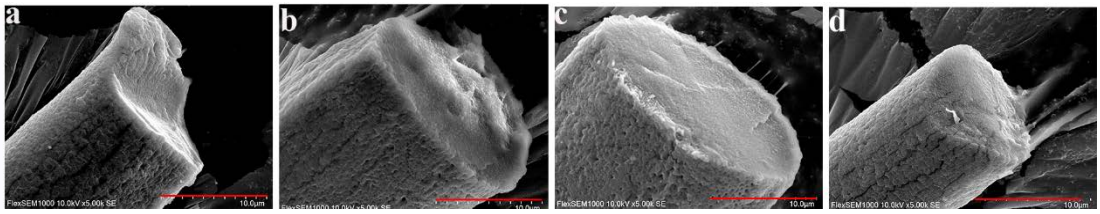

Figure 5: Cross-section morphology of different concentration of methanol coagulation bath spinning fibers. a: V(Methanol)/ V(Total)=1:2, b: V(Methanol)/ V(Total)=1:5, c: V(Methanol)/ V(Total)=1:10, d: V(Methanol)/ V(Total)=1:50. The scal bar was 10μm in SEM of cross-section.

3.3. Variability of protein secondary structure

Preprints (www.preprints.org) | NOT PEER-REVIEWED | Posted: 24 October 2022 doi:10.20944/preprints202210.0354.v1

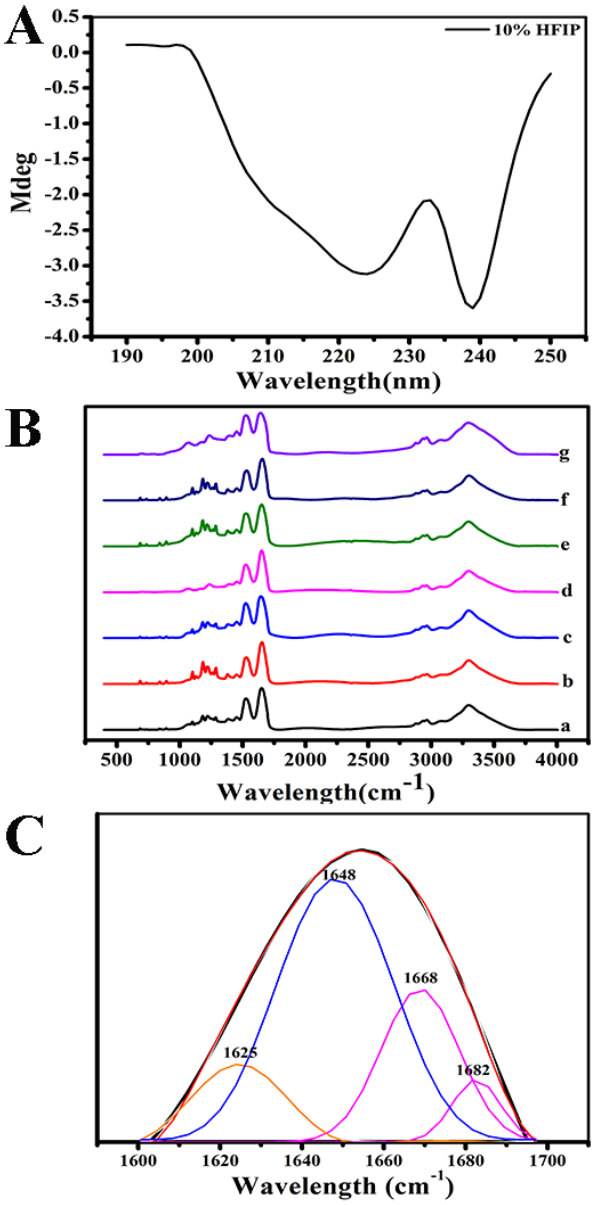

Figure 6: A: CD in 10% HFIP spinning dope. B: FTIR of different concentration of coagulation bath spinning fibers. C: Peak fitting of amide I. a: V(Methanol)/ V(Total)=1:2, b: V(Methanol)/ V(Total)=1:5, c: V(Methanol)/ V(Total)=1:10, d: V(Methanol)/ V(Total)=1:50, e: V(Methanol)/ V(Total)=1:100, f: V(Methanol)/ V(Total)=1:100, g: V(Methanol)/ V(Total)=1:100.

Table 2: The content of protein secondary structure in different fibers.

Content (%)	β-sheet	β-turn	random coil	α-helix
CD	21.5	12.1	20.8	45.6
a	12.96	28.78	58.26	
b	12.89	28.86	58.25	
c	12.9	28.85	58.25	
d	12.9	28.84	58.26	
e	12.9	28.85	58.25	
f	8.14	42.39	49.47	
g	12.9	28.8	27.73	30.57

Preprints (www.preprints.org) | NOT PEER-REVIEWED | Posted: 24 October 2022 doi:10.20944/preprints202210.0354.v1

Secondary structure changes of spinning fibers were analysis through FTIR, all spectra were normalized at 3275cm^{-1} (N-H stretching) for better visualization. All spinning fibers has no obvious differences, as shown in Figure 6B. Further analysis the protein secondary structure in amide I, 1605-1639 cm^{-1}, 1640-1650 cm^{-1}, 1650-1660 cm^{-1}, 1660-1670 cm^{-1}, attributed to β-sheet, random coil, α-helix, β-turn [19], respectively. When the spidroin powder dissolved in the 10% methanol analysis through circular dichroism (CD), the protein structure most was α-helix about 45.6%, β-sheet and random coil were less, contained 21.5% and 20.8%, respectively, the lest was β-turn contained 12.1% (Figure 6A and Table 2). During spinning process, the α-helix structure was disappeared, the random coil come into prominence, β-turn increased while β-sheet decreased. Secondary stretching in air, still has no α-helix, random coil and β-sheet both decreased while β-turn increased. While stretching in 0.1% methanol, α-helix structure reappeared but decreased to 30.57%, the content of random coil was similar as the CD's, it may be indicated that most random coil transform to α-helix. The percentage of β-sheet recovered to 12.9% while β-turn recovered to 28%. Totally, there were basically no differences in the secondary structure content of the fibers in the as-spun fibers, the secondary stretching both in air and in methanol have a different structure compared to other fibers.

3.4. Thermal stability

To evaluate the thermal properties of the fiber, thermogravimetric analysis was used to determine the weight loss rate. Due to the silk fiber was slight we assemble all seventh fibers together to perform the thermogravimetric test. The curve of the result was single, as shown in Figure 7, as the temperature start to heat till 100 ℃, the weight loss was 5%. The second stage was a slow thermal decomposition stage occurred between 100 ℃ and 240 ℃, the weight loss 10%. This means the silk fiber has thermal stability assumed that there is no clear thermal degradation before 200 ℃. Change occurred in the third stage, 240 ℃ to 363 ℃, where a rapid weight loss was observed. This may due to the breakage of peptide bonds and side groups of fiber the protein structure [12]. Then it returned to a gentle decline during 363 ℃ to 600 ℃.

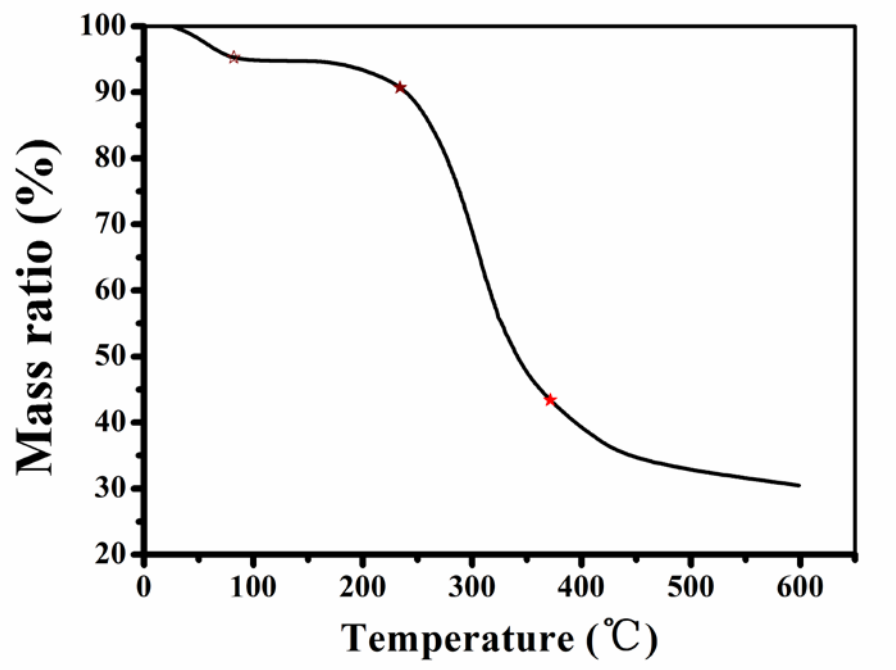

3.5. Mechanical properties of fibers

When the fiber just continuously spinning from the coagulation bath, the engineering strain of the fiber was relatively small, less than 10%. As lower the concentration of methanol, the maximum strain begins to increased, but there were still fibers with

Preprints (www.preprints.org) | NOT PEER-REVIEWED | Posted: 24 October 2022 doi:10.20944/preprints202210.0354.v1

small strain (Figure 7A). Secondary stretching in two different conditions, air and 0.1% methanol, resulted in different strain changes. Second stretching in air, all fibers' strain increased, the maximum strain of some fibers can increase to 250%, while most fibers still have a poor strain less than 100%. When stretching in 0.1% methanol, most fibers' strain increased over 100%, maximum strain up to 300%, but the stress was decreased compared to the fibers without stretching.

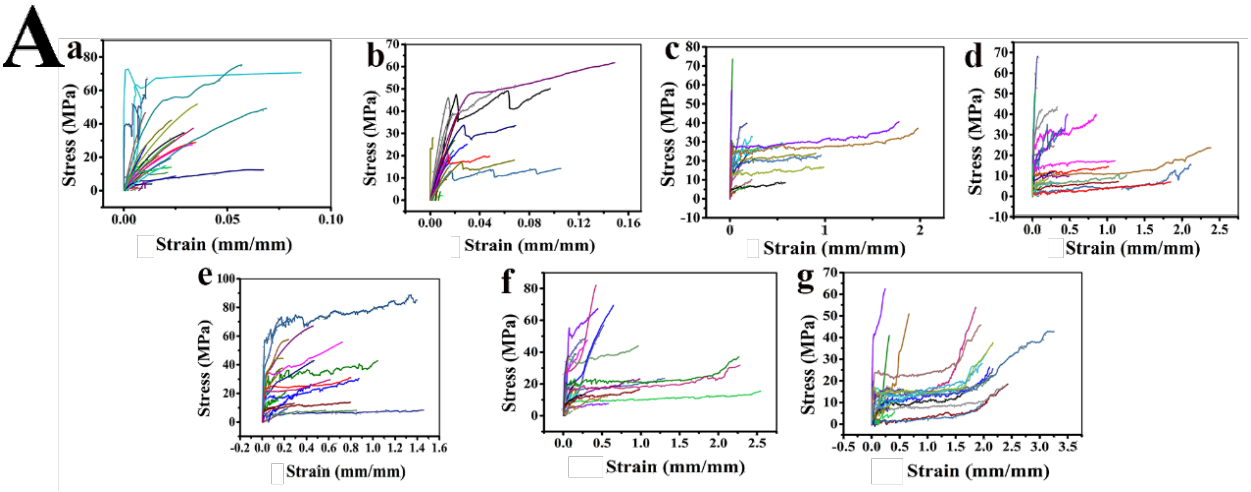

As shown in Figure 7B, fibers spun in 1:5 ($V_{methanol}/V_{total\ volume}$) has the highest modulus, which was about 3.052 GPa, the modulus of the fiber has significant difference compared with the fibers spun in 1:10 and 1:50 (V methanol/V total volume), and 1:10 also has significant difference compared with 1:50 and 1:100 (V methanol/V total volume), but the secondary stretching fiber have no difference in the coagulation bath of the same concentration of 1:100. The engineering stress of all fibers have no difference ($p>0.05$) (Figure 7C). The strain between fibers spun in 1: 2 and 1:5, 1:10 and 1:50 (V methanol/V total volume) both have no difference, but between 1:2, 1:5 and 1:10, 1:50, 1:100 has difference ($0.05<p<0.01$). While the fiber in the 1:100 (V methanol/V total volume) and stretching in air has no difference ($p>0.05$), but they have difference compared to secondary stretching in 0.1% methanol fibers ($0.05<p<0.01$) (Figure 7D). Therefore, the conclusion is that the concentration of coagulation bath methanol has influence on the fiber's strain and Young 's modulus, but cannot influence the fiber's stress.

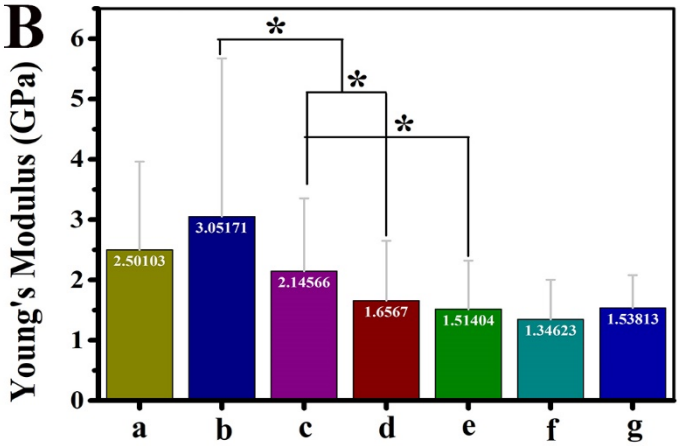

Preprints (www.preprints.org) | NOT PEER-REVIEWED | Posted: 24 October 2022 doi:10.20944/preprints202210.0354.v1

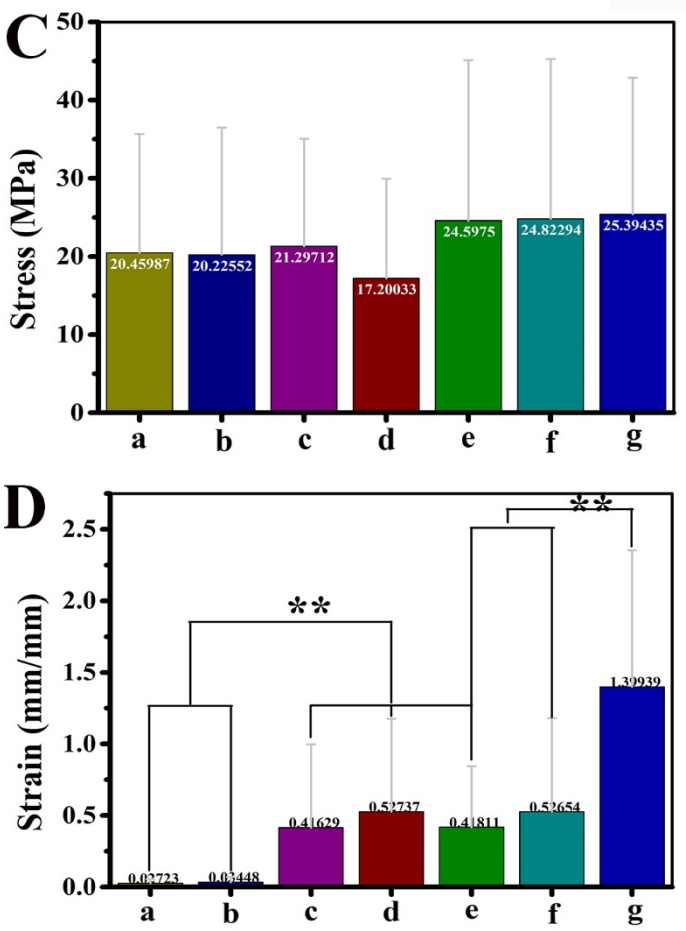

Figure 7: A: The strain-stress of different coagulation bath fiber. B: The significance analysis of different fiber's modulus. C: The significance analysis of different fiber's stress. D: The significance analysis of different fiber's strain. a: V(Methanol)/ V(Total)=1:2, b: V(Methanol)/ V(Total)=1:5, c: V(Methanol)/ V(Total)=1:10, d: V(Methanol)/ V(Total)=1:50, e: V(Methanol)/ V(Total)=1:100, f: V(Methanol)/ V(Total)=1:100 and secondary stretching in air, g: V(Methanol)/ V(Total)=1:100 and secondary stretching in 0.1% methanol.

Stretching promotes the re-alignment of the protein chains, which can be frozen by re-establishing the hydrogen bond network, especially in simulating the tensile properties of spider silk [4]. The mechanical properties of secondary stretching fibers are greater than those of no stretching fibers, which can be attributed to the degree of molecular orientation and parallel arrangement of aggregated secondary structures, which leads to less slippage of chains under loading. As the fiber is stretching and lengthened, the physical interactions among polymer chains and secondary structures become untangled and more closely arranged [18].

4. Conclusion

The wet spinning of recombinant Pyriform repeat domain spidroin was tried. HFIP was selected as the spinning solvent, and the concentration of coagulation bath methanol was examined. Two-step stretching, stretching in air and in 1% methanol, gave a higher engineering strain. This indicated that high water content is presumably responsible for improved strain of the fiber spun from the coagulation bath. Secondary stretching is necessary for mechanical of the fiber. Stretching in 1% methanol can obtained higher strain fiber than in air, furthermore the α-helix contained in the former fiber but not in the latter. The concentration of coagulation bath has slight effect on chemical structure of spinning fibers.

Acknowledgement:

This work was supported by the Chinese National Natural Science Foundation [No. 31570721].
Key project of Shanghai Science and Technology Commission [No. 14521100700].

Reference:

[1] Dos Santos-Pinto JR, Garcia AM, Arcuri HA, Esteves FG, Salles HC, Lubec G, Palma MS. Silkomics: Insight into the Silk Spinning Process of Spiders. J Proteome Res. 2016 Apr 1;15(4):1179-93. doi: 10.1021/acs.jproteome.5b01056. Epub 2016 Mar 14.

[2] Kovoor J, Zylberberg L. Fine structural aspects of silk secretion in a spider (Araneus diadematus). I. Elaboration in the pyriform glands. Tissue Cell. 1980;12(3):547-56. doi: 10.1016/0040-8166(80)90044-0.

[3] Humenik M, Scheibel T, Smith A. Spider silk: understanding the structure-function relationship of a natural fiber. Prog Mol Biol Transl Sci. 2011;103:131-85. doi: 10.1016/B978-0-12-415906-8.00007-8.

[4] Guinea GV, Elices M, Pérez-Rigueiro J, Plaza GR. Stretching of supercontracted fibers: a link between spinning and the variability of spider silk. J Exp Biol. 2005 Jan;208(Pt 1):25-30. doi: 10.1242/jeb.01344.

[5] Lüken A, Geiger M, Steinbeck L, Joel AC, Lampert A, Linkhorst J, Wessling M. Biocompatible Micron-Scale Silk Fibers Fabricated by Microfluidic Wet Spinning. Adv Healthc Mater. 2021 Oct;10(20):e2100898. doi: 10.1002/adhm.202100898. Epub 2021 Jul 31.

[6] Rinoldi C, Costantini M, Kijeńska-Gawrońska E, Testa S, Fornetti E, Heljak M, Ćwiklińska M, Buda R, Baldi J, Cannata S, Guzowski J, Gargioli C, Khademhosseini A, Swieszkowski W. Tendon Tissue Engineering: Effects of Mechanical and Biochemical Stimulation on Stem Cell Alignment on Cell-Laden Hydrogel Yarns. Adv Healthc Mater. 2019 Apr;8(7):e1801218. doi: 10.1002/adhm.201801218. Epub 2019 Feb 6.

[7] Micsonai A, Wien F, Bulyáki É, Kun J, Moussong É, Lee YH, Goto Y, Réfrégiers M, Kardos J. BeStSel: a web server for accurate protein secondary structure prediction and fold recognition from the circular dichroism spectra. Nucleic Acids Res. 2018 Jul 2;46(W1):W315-W322. doi: 10.1093/nar/gky497.

[8] Bai X, Yuan W. [Formation of natural silk and progress in artificial spinning]. Sheng Wu Gong Cheng Xue Bao. 2020 Sep 25;36(9):1767-1778. Chinese. doi: 10.13345/j.cjb.200029.

[9] Yan J, Zhou G, Knight DP, Shao Z, Chen X. Wet-spinning of regenerated silk fiber from aqueous silk fibroin solution: discussion of spinning parameters. Biomacromolecules. 2010 Jan 11;11(1):1-5. doi: 10.1021/bm900840h.

[10] Miranda CS, Silva AFG, Pereira-Lima SMMA, Costa SPG, Homem NC, Felgueiras HP. Tunable Spun Fiber Constructs in Biomedicine: Influence of Processing Parameters in the Fibers' Architecture. Pharmaceutics. 2022 Jan 11;14(1):164. doi: 10.3390/pharmaceutics14010164.

[11] Heidebrecht A, Eisoldt L, Diehl J, Schmidt A, Geffers M, Lang G, Scheibel T. Biomimetic fibers made of recombinant spidroins with the same toughness as natural spider silk. Adv Mater. 2015 Apr 1;27(13):2189-94. doi: 10.1002/adma.201404234. Epub 2015 Feb 16.

[12] Zhao M, Qi Z, Tao X, Newkirk C, Hu X, Lu S. Chemical, Thermal, Time, and Enzymatic Stability of Silk Materials with Silk I Structure. Int J Mol Sci. 2021 Apr 16;22(8):4136. doi: 10.3390/ijms22084136.

[13] Asakura T, Matsuda H, Naito A, Abe Y. Formylation of Recombinant Spider Silk in Formic Acid and Wet Spinning Studied Using Nuclear Magnetic Resonance and Infrared Spectroscopies. ACS Biomater Sci Eng. 2022 Jun 13;8(6):2390-2402. doi: 10.1021/acsbiomaterials.2c00151. Epub 2022 May 9.

[14] Blasingame E, Tuton-Blasingame T, Larkin L, Falick AM, Zhao L, Fong J, Vaidyanathan V, Visperas A, Geurts P, Hu X, La Mattina C, Vierra C. Pyriform spidroin 1, a novel member of the silk gene family that anchors dragline silk fibers in attachment discs of the black widow spider, Latrodectus hesperus. J Biol Chem. 2009 Oct 16;284(42):29097-108. doi: 10.1074/jbc.M109.021378. Epub 2009 Aug 7.

[15] Simmons JR, Xu L, Rainey JK. Recombinant Pyriform Silk Fiber Mechanics Are Modulated by Wet-Spinning Conditions. ACS Biomater Sci Eng. 2019 Oct 14;5(10):4985-4993. doi: 10.1021/acsbiomaterials.9b00504. Epub 2019 Sep 26.

[16] Rising A, Johansson J. Toward spinning artificial spider silk. Nat Chem Biol. 2015 May;11(5):309-15. doi: 10.1038/nchembio.1789. Epub 2015 Apr 17.
[17] Wolff JO, Grawe I, Wirth M, Karstedt A, Gorb SN. Spider's super-glue: thread anchors are composite adhesives with synergistic hierarchical organization. Soft Matter. 2015 Mar 28;11(12):2394-403. doi: 10.1039/c4sm02130d.
[18] Jao D, Hu X, Beachley V. Bioinspired Silk Fiber Spinning System via Automated Track-Drawing. ACS Appl Bio Mater. 2021 Dec 20;4(12):8192-8204. doi: 10.1021/acsabm.1c00630.
[19] De Meutter J, Goormaghtigh E. Evaluation of protein secondary structure from FTIR spectra improved after partial deuteration. Eur Biophys J. 2021 May;50(3-4):613-628. doi: 10.1007/s00249-021-01502-y. Epub 2021 Feb 3.
[20] Zhang J, Jia Q, Meng E, Meng Q. Characteristics of electrospun membranes in different spidroin/PCL ratios. Biomed Mater. 2021 Oct 13;16(6). doi: 10.1088/1748-605X/ac2ab7.